0013-7227/08/$15.00/0
Printed in U.S.A.

Endocrinology 149(3):1113–1120

doi: 10.1210/en.2007-0412

Cooperative Binding of Insulin-Like Peptide 3 to a Dimeric Relaxin Family Peptide Receptor 2

Angela Manegold Svendsen, Milka Vrecl, Tina M. Ellis, Anders Heding, Jesper Bøggild Kristensen, John D. Wade, Ross A. D. Bathgate, Pierre De Meyts, and Jane Nøhr

Receptor Systems Biology Laboratory (A.M.S., T.M.E., P.D.M., J.N.), Hagedorn Research Institute, DK-2820 Gentofte, Denmark; Institute of Anatomy, Histology, and Embryology (M.V.), Veterinary Faculty, University of Ljubljana, Sl-1000 Ljubljana, Slovenia; 7TM Pharma A/S (A.H.), DK-2970 Hørsholm, Denmark; Chemical API Supply Isotopes (J.B.K.), Novo Nordisk, DK-2760 Måløv, Denmark; and Howard Florey Institute of Experimental Physiology and Medicine (J.D.W., R.A.D.B.), University of Melbourne, Victoria 3010, Australia

Insulin-like peptide 3 (INSL3) binds to a G protein-coupled receptor (GPCR) called relaxin family peptide receptor 2 (RXFP2). RXFP2 belongs to the leucine-rich repeat-containing subgroup (LGR) of class A GPCRs. Negative cooperativity has recently been demonstrated in other members of the LGR subgroup. In this work, the kinetics of INSL3 binding to HEK293 cells stably transfected with RXFP2 (HEK293-RXFP2) have been investigated in detail to study whether negative cooperativity occurs and whether this receptor functions as a dimer. Our results show that negative cooperativity is present and that INSL3-RXFP2 binding shows both similarities and differences with insulin binding to the insulin receptor. A dose-response curve for the negative cooperativity of INSL3 binding had a reverse bell shape reminiscent of that seen for the negative cooperativity of insulin binding to its receptor. This suggests that binding of INSL3 may happen in a *trans* rather than in a *cis* way in a receptor dimer. Bioluminescence resonance energy transfer ($BRET^2$) experiments confirmed that RXFP2 forms constitutive homodimers. Heterodimerization between RXFP2 and RXFP1 was also observed. (*Endocrinology* 149: 1113–1120, 2008)

THE INSULIN-LIKE PEPTIDE 3 (INSL3) is a member of the insulin/relaxin-related gene family (1, 2), and binds to the relaxin family peptide receptor 2 (RXFP2) (formerly called LGR8). In humans, the insulin-related gene family includes the genes for insulin, IGF-I and -II, relaxins (H1, H2, and H3), and INSL3, -4, -5, and -6 (3, 4). Proteins of this superfamily are synthesized as prepro-proteins consisting of four domains (pre, B, C, and A). These are then processed by proteolytic removal of the pre domain and in some case the C domain and fold to form mature proteins, in which the A and B domains are covalently linked by two disulfide bonds (5). The peptide hormones and growth factors of this gene family play a fundamental role in the control of essential cellular and physiological processes such as survival or apoptosis, cell migration, cell cycle, proliferation and differentiation, and body growth, metabolism, reproduction, and longevity (6).

Despite differences in the relaxins of different species, all relaxins share key structural features such as the general size (6000 Da), the canonical insulin-type disulfide bridges and chain structure, three preserved glycines, one in the A chain and two in the B chain, and the arginine residues Arg^{B13} and Arg^{B17} (H2 human relaxin numbering) (7–9). More significantly, the amino acid sequences of relaxins of 23 different species contain an eight-amino-acid sequence in the B chain that has been conserved in evolution. This sequence, postulated to represent the receptor recognition and binding site region, has the motif Arg-X-X-X-Arg-X-X-Ile/Val. The spacing between and the location of the arginine residues in this region is thought to be critical for receptor binding. The human INSL3 peptide similarly contains the same spacing between arginine residues (Arg-X-X-X-Arg motif); however, their positions have been displaced by four amino acids toward the C terminus from the corresponding position within relaxin (10). Recent studies have shown that Arg^{B16}, Trp^{B27}, and Val^{B19} (human INSL3 numbering) are the key residues of INSL3 that are responsible for the interaction with the ectodomain of RXFP2, whereas His^{B12} and Arg^{B20} play a secondary role (11). In INSL3, a distinct motif (Gly-Gly-Pro-Arg-Trp) was identified at a B chain C-terminal sequence that was also involved in RXFP2 binding. The Trp residue is essential but not sufficient for receptor binding, and the proline residue is likely important for maintaining the correct conformation (12).

The receptors for INSL3, as well as those for relaxins H1–2, together with the glycoprotein hormone receptors (LH receptor, FSH receptor, and TSH receptor), belong to the leucine-rich repeat-containing subgroup (LGR) of the rhodopsin-like G protein-coupled receptor (GPCR) superfamily (class A). The receptors for INSL4 and INSL6 are unknown. INSL3 binds to the RXFP2 receptor. This subgroup contains an extracellular domain with multiple leucine-rich repeats and a GPCR transmembrane domain. The type C subgroup, to which RXFP2 belongs, is distinct from LGR subtype A and

First Published Online December 6, 2007

Abbreviations: BRET, Bioluminescence resonance energy transfer; CG, chorionic gonadotropin; GFP, green fluorescent protein; GPCR, G protein-coupled receptor; INSL3, insulin-like peptide 3; LGR, leucine-rich repeat-containing subgroup; NK1R, neurokinin type 1 receptor; RXFP2, relaxin family peptide receptor 2; WT, wild type.

***Endocrinology* is published monthly by The Endocrine Society (http://www.endo-society.org), the foremost professional society serving the endocrine community.**

B in having an N-terminal low-density lipoprotein receptor-like cysteine-rich motif and a unique hinge region. Similar to the type A LGRs, which include the glycoprotein hormone receptors, the ectodomain of RXFP2 functions as the ligand-binding domain, where ligand binding leads to the activation of adenylyl cyclase and the protein kinase A-dependent pathway in target tissues (13).

The RXFP2 receptor has been proposed to contain two binding sites, which have significantly different affinities. The high-affinity site is located in the ectodomain, whereas the low-affinity site is located upon the transmembrane segment of the receptor, likely within exoloop 2 (12, 14). The high-affinity binding site couples to cAMP signaling with high efficiency, whereas the low-affinity site couples with lower efficiency. At the same time, the primary site (high-affinity site) dictates receptor binding characteristics, although the lower affinity site also exerts some influence and modulates ligand affinity for the primary site (15).

Following classical studies on the insulin receptor (16, 17), negative cooperativity (18, 19) shown by curvilinear Scatchard plots and accelerated dissociation of the tracer-receptor complex in the presence of unlabeled ligand, has been demonstrated in β_2-adrenergic (20) and TSH receptor (21) binding in the early 1970s, before they were shown to be GPCRs. That issue, however, became contentious (22, 23) especially because the GPCRs were for a long time thought to be monomeric. However, recent evidence has accumulated using, among others, bioluminescence resonance energy transfer (BRET), that the majority of GPCRs do form homodimers and heterodimers (24, 25). In that context, a clear link between homodimerization and negative cooperativity was recently demonstrated for glycoprotein hormone receptors (including TSH receptors), which are other members of the LGR subgroup (26).

In this study, we investigated whether INSL3 binding to RXFP2 exhibits negative cooperativity and whether RXFP2 forms homo- and heterodimers.

Materials and Methods

Chemicals and reagents

Cell culture reagents, fetal bovine serum, transfection lipids and antibiotics were purchased from Invitrogen (Taastrup, Denmark). Chemicals were purchased from Sigma (Copenhagen, Denmark).

Synthetic human INSL3 was purchased from Phoenix Pharmaceuticals, Inc. (Belmont, CA), recombinant H2 relaxin was kindly provided by BAS Medical (San Mateo CA), and synthetic H3 relaxin was provided by J. D. Wade.

Cell culture

HEK293 cells obtained from the European Collection of Animal Cell Cultures (Salisbury, UK) and HEK293 cells stably transfected with RXFP2 (HEK293-RXFP2) (27), were cultured in RPMI 1640 with 10% fetal bovine serum, 2 mM L-glutamine, and 100 U/ml penicillin-streptomycin at 37 C in a humidified atmosphere of 5% (vol/vol) CO_2. For the stable transfectants, zeocin (200 μg/ml) was added once a week.

Vector construction

Human cDNAs of RXFP1 and RXFP2 (27) were cloned into pcDNA3.1 (+/−) vectors (Invitrogen) containing either Rluc or green fluorescent protein (GFP^2) inserts using standard molecular biology methods. The Rluc and GFP^2 inserts were fused in frame to the C terminus of the receptors. The C-terminally GFP^2-tagged neurokinin type 1 receptor (NK1R) and two membrane-inserted GFP^2-tagged constructs were generated (14aa GFP^2 and GFP^2 17aa). The 14aa GFP^2 construct contains 14 amino acids residues from p59Fyn inserted at the N-terminal end of GFP^2. The GFP^2 17aa construct contains 17 amino acids residues from K-ras inserted at the C-terminal end of GFP^2. Both the N-terminal sequence of Fyn and the C-terminal sequence of K-ras were previously shown to direct a native protein to the plasma membrane (28, 29). The 14aa GFP^2 and GFP^2 17aa cDNAs were kindly provided by Dr. Rasmus Jørgensen (7TM Pharma A/S, Hørsholm, Denmark). All clones were verified by sequencing.

Labeling of INSL3

INSL3 from Phoenix Pharmaceuticals was labeled in a stoichiometric radioiodination protocol to yield monoiodinated tracer (30) essentially as described by Buellesbach and Schwabe (8, 31). For a more detailed protocol, see supplemental data, published on The Endocrine Society's Journals Online web site at http://endo.endojournals.org.

Receptor binding assays

All experiments were done three times in duplicate unless otherwise stated.

Association assays

[^{125}I]INSL3 and HEK293-RXFP2 cells were incubated at 4, 15, 26, or 37 C for different time intervals. Specific INSL3 binding was determined by centrifugation as previously described (32). Two additional aliquots were not centrifuged but counted as total.

Competition assays were done as described before (32). HEK293-RXFP2 cells were incubated with a constant amount of [^{125}I]INSL3 and increasing concentrations of unlabeled ligand (INSL3 or H2 or H3 relaxin) at 15 C for 2.5 h. This was done in buffer with pH 6.0 or 7.6. Duplicate aliquots were centrifuged after incubation and the bound activity counted. Two additional aliquots were not centrifuged but counted as total.

Dissociation assays were performed as described (16). [^{125}I]INSL3 and HEK293-RXFP2 cells were preincubated. After 2 h of incubation, the cells were resuspended in an equal amount of buffer. Duplicate aliquots were diluted 40-fold in the absence and presence of a constant amount of unlabeled INSL3 and incubated at 4, 15, or 37 C. After different time intervals, the cells were centrifuged and the bound activity counted. Two additional aliquots were not centrifuged but counted as total. In a second experiment, duplicate aliquots were diluted 40-fold with increasing concentrations of unlabeled ligand (INSL3 or H2 or H3 relaxin) for a constant amount of time.

$BRET^2$ experiments were performed as described (33–35). For $BRET^2$ saturation experiments, HEK293 cells were cotransfected with a constant amount of vectors coding for Rluc-tagged receptors and increasing amounts of vectors coding for GFP^2-tagged receptors or with a constant amount of RXFP2 Rluc with increasing amounts of NK1R GFP^2, 14aa GFP^2 or GFP^2 17aa (control experiments). For $BRET^2$ competition assays, HEK293 cells were cotransfected with a constant amount of Rluc- and GFP^2-tagged receptors and increasing amounts of untagged receptor. For the heterodimerization experiments, HEK293 cells were cotransfected with constant amounts of RXFP2 Rluc and RXFP1 GFP^2 or with RXFP2 Rluc and increasing amounts of RXFP2 TM1–7 GFP^2.

Expression levels of Rluc- and GFP^2-tagged constructs for each $BRET^2$ experiment were monitored by luminescence and fluorescence measurements as described (34).

Confocal fluorescence microscopy

Confocal microscopy experiments were performed as described earlier (36). Briefly, HEK293 cells transfected with either 14aa GFP^2 or GFP^2 17aa were examined under an oil immersion objective (×40) using a Leica multispectral confocal laser microscope (Leica TCS NT, Heidelberg, Germany). Detection of the GFP^2-tagged 14aa and 17aa constructs and nuclei labeled with TO-PRO-3 signals was achieved with the use of excitation line lasers at 488 nm (argon) and 633 nm (helium-neonium). The data from the channels were collected with 4-fold averaging at a

resolution of 1024 × 1024 pixels. Optical sections (1.0 μm) were taken and representative sections corresponding to the middle of the cells are presented using Adobe Photoshop 7.0 computer software.

Statistical analysis

All results are the means of duplicate determinations in three independent experiments unless otherwise stated.

Association data. The average values of the double determinations were analyzed by a three-way ANOVA model with random effects. The effects of experiment, temperature, time, and the interaction between time and temperature were considered as fixed effects, and the interaction between experiment and temperature was considered as random (*i.e.* observations at different time points from the same temperature and experiment are correlated).

Dissociation data. The results from time = 300 min and time = 1440 min were analyzed statistically. The average values of the double determinations were calculated, and the difference between buffer alone and added INSL3 was constructed, yielding three differences from each temperature. The differences were analyzed by a one-way ANOVA with temperature as the fixed factor.

Affinity data. The K_d values from three different experiments at pH 7.6 and pH 6.0 were compared using a paired *t* test.

Effect of accelerated dissociation data. Data were analyzed by a three-way ANOVA model (ANOVA) with random effects. The effects of the three experiments, the treatments (INSL3, H2 relaxin, or H3 relaxin), the concentration of the unlabeled ligand, and the interaction between the concentration and the treatments were considered as fixed effects. The interaction between the three experiments and the treatments was considered as random.

BRET^2 saturation data (RXFP2 Rluc/RXFP2 GFP^2 pair and RXFP2 Rluc/RXFP2 TM1–7 GFP^2 pair). The average values of the six replicate terminations were analyzed by a three-way ANOVA model with random effects. The effects of three experiments, stimulation with 0, 1.6, or 10 nM INSL3 and of the GFP^2/Rluc ratio were considered as fixed effects, and the interaction between three experiments and stimulation was considered as random.

Statistical analysis of the data of Fig. 5, B and C, could not be performed because it is not possible to get the same GFP/Rluc ratio in different experiments when performing cotransfection studies. However, the findings are consistent with what has been shown before in other BRET experiments (26, 33).

Heterodimerization experiment. From each of three experiments, six replicate values with RXFP1 and RXFP2 were obtained. When data from each experiment were analyzed separately (two-sample *t* test), the difference was significantly different from zero in two of the three experiments. In a combined analysis, the overall difference was not significantly different from zero.

Results and Discussion

Temperature dependence of INSL3 association and dissociation

The binding of INSL3 to RXFP2 showed clear temperature dependence with a faster association at higher temperatures (Fig. 1). The interaction between time and temperature was strongly significant; thus, the curves from different temperatures cannot be considered identical. Interestingly, the equilibrium reached the same level at all temperatures, indicating that both the association and dissociation are faster and compensate for each other at higher temperatures. The binding of insulin to the insulin receptor also showed temperature dependence for association with faster association at higher temperatures, but the dissociation rate was more sensitive to temperature, generating a decreased equilibrium binding at higher temperatures (32).

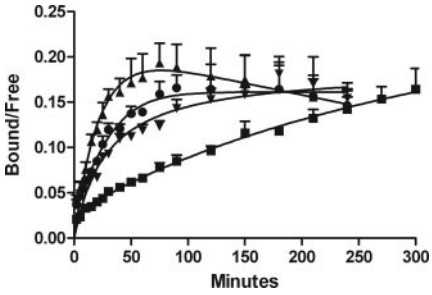

FIG. 1. INSL3 binding/association assay. Association of [^{125}I]INSL3 at 4 C (■), 15 C (▼), 26 C (●), and 37 C (▲). Bound/free [^{125}I]ligand is plotted as a function of time. There is a clear temperature dependence of association, *i.e.* the higher the incubation temperature, the faster the association. At 4 C, the association started very slowly, and after 300 min, steady state was not reached yet. It took approximately 2.5, 1.5, and 1 h at 15, 26, and 37 C, respectively, to reach steady state binding. All steady-state binding reached the same level.

The dissociation of [^{125}I]INSL3 from RXFP2 was indeed also affected by temperature with an increasing rate of dissociation with increasing temperatures (Fig. 2). The presence of unlabeled ligand enhanced the radioligand dissociation significantly at all temperatures studied. The difference between added INSL3 and buffer alone was significantly different at all temperatures at time = 300 min, but not at 37 C at time = 1440 min. However, at 4 C, the presence of unlabeled INSL3 did not affect the rate of [^{125}I]INSL3 dissociation for at least 3 h of dissociation. This could be due to the very slow binding of INSL3 to RXFP2 at this temperature. Limbird and Lefkowitz (37) showed a similar temperature dependence of both association and dissociation of alprenolol to the β_2-adrenergic receptor, where the association curves also reached the same level of steady-state binding at the different temperatures. Also, in the case of the β_2-adrenergic receptor, the addition of unlabeled ligand accelerated the dissociation of labeled ligand at all temperatures, although at 4 C, the presence of unlabeled ligand did not affect the dissociation

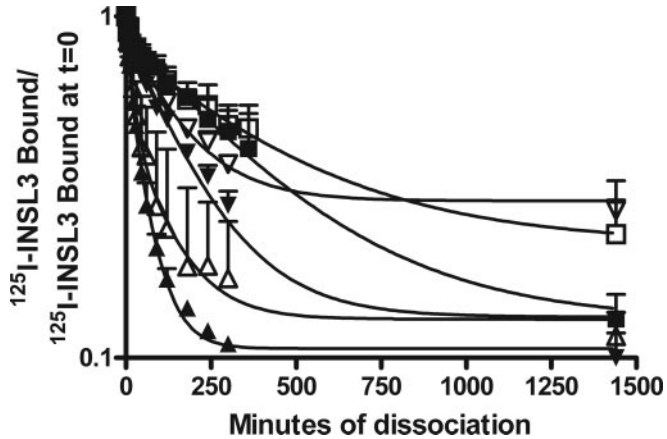

FIG. 2. Dissociation assay of INSL3 from RXFP2. Bound tracer at time t divided by bound tracer at time 0 was plotted as a function of time. Dissociation of [^{125}I]INSL3 at 4 C (■), 15 C (▼), and 37 C (▲), with (*closed symbols*) and without (*open symbols*) addition of unlabeled ligand. At 4 C, the dissociation is very slow, and the addition of 160 nM unlabeled INSL3 accelerates the dissociation only slightly, but still enough to indicate the presence of negative cooperativity. The fastest dissociation was seen at 37 C.

rate for at least 60 min. This slow onset of effect contrasts with the insulin receptor, where the accelerating effect of unlabeled ligand is observed within minutes, as also seen for the TSH receptor (21, 26). This suggests that the rate constants within the dimers in the various systems are different and warrants mathematical modeling for measuring those constants. The dissociation of insulin is also temperature dependent with a faster dissociation at higher temperatures (Fig. 9 in Ref. 17). The dissociation by dilution plus unlabeled insulin was also accelerated by increasing temperatures, but to a lesser extent than dilution only; as a result, the difference between dilution only and dilution plus unlabeled ligand decreased markedly with increased temperature (17). The opposite is seen with INSL3, where the difference between the dilution only and dilution plus unlabeled INSL3 gets bigger with increasing temperatures (Fig. 2).

In addition to the temperature dependence, the pH dependence of binding and dissociation was investigated. For results, see supplemental data.

Affinity of INSL3/RXFP2 binding

Consistent with the previous proposal that RXFP2 has two binding sites (12), two K_d values were estimated by computer curve-fitting of competition curves. The K_d values of the high- and low-affinity sites were 0.100 ± 0.020 and 0.310 ± 0.080 nM, respectively (at pH 7.6), using a sequential model. The K_d was 0.227 ± 0.050 nM using a one-site model (Fig. 3A). Halls *et al.* (12) reported a curved Scatchard plot with K_d of 0.58 ± 0.014 nM and 4.47 ± 0.161 nM for the high- and low-affinity sites. However, these results relate to binding of [^{33}P]H2 relaxin to RXFP2 and not [^{125}I]INSL3.

Furthermore, we examined whether the difference in pH had an impact on the K_d values of INSL3. INSL3 had a significantly higher affinity toward RXFP2 at pH 6.0 in comparison with pH 7.6, in agreement with the pH dependence curve (K_d values 0.156 ± 0.008 nM, one-site model, or 0.073 ± 0.005 and 0.260 ± 0.080 nM, sequential model).

H2 and H3 relaxin had a much decreased potency in competing for [^{125}I]INSL3 binding to RXFP2 (K_d = 381 ± 36 and 400 ± 31 nM, respectively) (Fig. 3B). This could be due to the different binding motifs in the B chain of the hormone. Interestingly, both RXFP1 and RXFP2 bind H2 relaxin (10), which implies that the ligand-binding domain of both receptors must share some similarity, whereas the ligands themselves have subtle differences, which affords them their specificity. The potency of H2 binding to RXFP2 using [^{125}I]INSL3 as a tracer in this study is much weaker than that previously found using [^{33}P]H2 relaxin as a tracer on the same receptor (K_d = 1.062 ± 0.127 nM) (12). The importance of INSL3 His^{B12}, Arg^{B16}, Val^{B19}, and Arg^{B20} has been shown before (11). Those residues comprise a relaxin-like binding cassette in INSL3. However, unlike relaxin binding to RXFP1, the Trp^{B27} residue is essential for high-affinity binding of INSL3 to RXFP2. This could explain why H2 relaxin competes with [^{33}P]H2 relaxin with high affinity but only with low affinity for [^{125}I]INSL3. It has recently been shown that H3 relaxin binds to RXFP2, although with low affinity, but that binding does not stimulate cAMP accumulation in human RXFP2-expressing cells at concentrations up to 1 μM (14, 27). This is consistent with the very high K_d; however, H3 relaxin is known to stimulate cAMP production in cells expressing RXFP1 (12). That H3 relaxin binds to RXFP1 with high affinity but low affinity to RXFP2 could also be due to differences in the binding motifs.

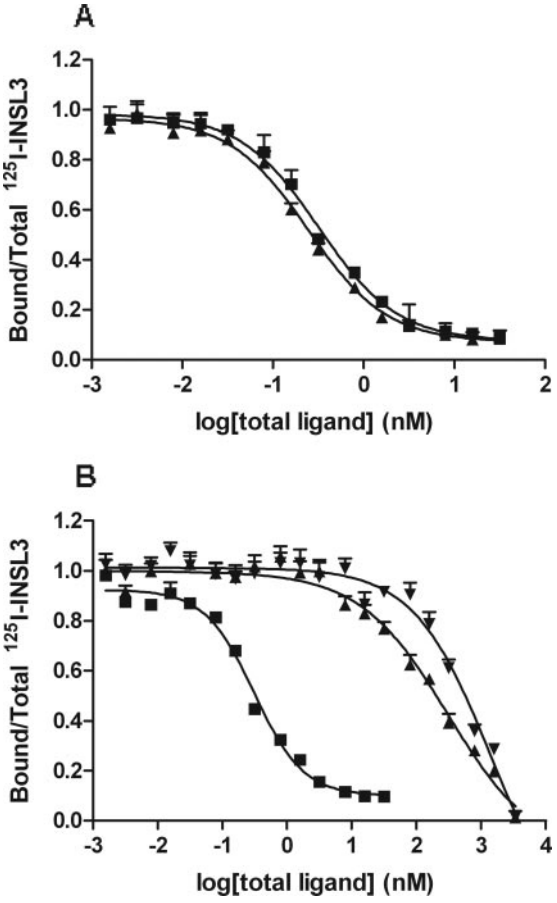

FIG. 3. Homologous and heterologous competition assays. All curves are plotted as bound/total labeled INSL3 as a function of the logarithm of the concentration of unlabeled ligand. A, Homologous competition assay with labeled and unlabeled INSL3 at pH 6.0 (▲) and 7.6 (■). INSL3 had a significantly higher affinity toward RXFP2 at pH 6.0 in comparison with pH 7.6, in agreement with the pH dependence curve. B, Heterologous competition assay with unlabeled INSL3 (control, ■), unlabeled H2 (▲), and H3 relaxin (▼). The curves of both H2 and H3 relaxin were markedly shifted to the right, and both hormones have a much lower affinity to RXFP2 than INSL3 at 15 C and pH 7.6.

Negative cooperativity in INSL3/RXFP2 binding

The concept of negative cooperativity of insulin binding to the insulin receptor has been investigated and documented for more than 30 yr (17, 38, 39). This was usually done by measuring ligand-accelerated tracer dissociation in an infinite dilution. Also in the case of INSL3, the addition of unlabeled hormone accelerated the dissociation of the prebound tracer (Fig. 2). However, this effect is quantitatively different from insulin dissociation in that the effect develops slowly and continues over time, whereas with insulin, the effect is observed to be very fast. Like insulin's, dissociation of INSL3 from RXFP2 is not first order. Dose-response curves for the accelerated dissociation are bell-shaped (self-antag-

onism) and show a loss of the dissociation acceleration at INSL3 concentrations of more than 500 nM (Fig. 4). Higher concentrations of unlabeled ligand could not be used due to limited access to the ligand. However, the experiment has been performed three times, and the findings have been reproducible. Both H2 and H3 relaxin showed a much decreased potency of accelerated dissociation, consistent with the much higher K_d values. The interaction between the treatment and the concentration of the unlabeled ligand was strongly significant; thus, the three sets of curves from different ligands cannot be considered identical. However, the curves from H2 relaxin and H3 relaxin were not significantly different. The same phenomenon as with INSL3 has been observed with insulin binding to the insulin receptor (38, 39). However, the time course for the development of the dose-response curve for negative cooperativity takes a much longer incubation time to achieve the full effect for accelerated dissociation in the case of INSL3 binding than for insulin binding. Furthermore, the maximal effect for accelerated dissociation is less for INSL3 (at maximal effect, 70% is still bound) than for insulin. The occurrence of negative cooperativity, shown by the accelerated dissociation of the ligands, suggests that the RXFP2 receptor exists as a dimer or oligomer rather than a monomer, and the bell-shaped dose-response curve for negative cooperativity of INSL3 binding to RXFP2 suggests that the two binding sites cross-linking may happen in a *trans* rather than in a *cis* way like in the case of the insulin receptor, as has been proposed before (12). This could be explained by the fact that RXFP2 has one high- and one low-affinity binding site (called binding sites 1 and 2). At low concentrations, INSL3 binds with high affinity by cross-linking sites 1 and 2 of two different molecules, leaving the second pair of binding sites unoccupied (Fig. 1B in Ref. 40). On partial dissociation of the first bound INSL3 molecule and at increasing concentrations of INSL3, a second INSL3 molecule binds and cross-links the vacant binding sites 1 and 2, accelerating the dissociation of the prebound INSL3. This phenomenon is lost at concentrations above 500 nM, because of the binding of two INSL3 molecules to the empty sites, thus preventing a second cross-link of the subunits. This would explain the bell-shaped dose-response curve of dissociation kinetics (37). In the *cis*-binding way, the peptide binds to the high-affinity site in the ectodomain and the low-affinity site at the 7TM domain in the same molecule of the dimer; in the *trans*-binding way, the peptide binds to the high-affinity site in the ectodomain in one molecule and the low-affinity site at the 7TM domain in the second molecule of the dimer. This *trans*-binding mechanism is consistent with what has been suggested previously for binding of chorionic gonadotropin (CG) to the LH receptor, but that receptor is capable of *cis* binding as well, which suggests transient interactions between the receptor pairs (40).

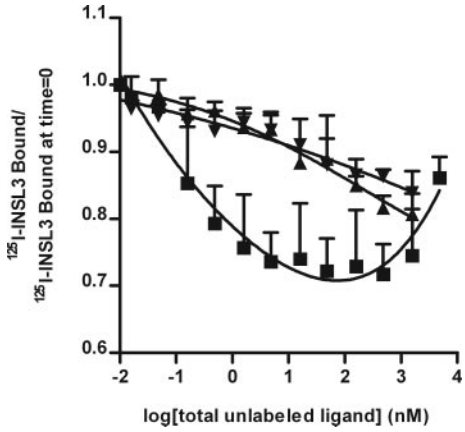

FIG. 4. Dose-response curve for negative cooperativity. Bound tracer after 7 h of incubation at 15 C divided by bound tracer at time 0 was plotted as a function of the logarithm of the concentration of the unlabeled ligand. To study the relative potency of the accelerated dissociation, homologous dose-response curves for negative cooperativity were performed, where a constant amount of labeled INSL3 is dissociated from RXFP2 as a function of increasing concentration of unlabeled INSL3 (■). The same experiment was repeated as a heterologous dose-response curve for negative cooperativity, where the same constant amount of labeled INSL3 is dissociated as a function of increasing concentration of unlabeled H2 (▲) or H3 (▼) relaxin. The curve for the homologous dose-response curve for negative cooperativity was inverse bell shaped. When examining the results of the heterologous experiments, it is seen that the curves in the presence of both H2 and H3 relaxin were shifted to the right in comparison with the INSL3 curve, and the maximal effect for accelerated dissociation is smaller. Furthermore, the curves for H2 and H3 relaxin seem not to be bell shaped, but this would probably demand higher concentrations.

Evidence for RXFP2 homo- and heterodimerization by BRET²

To verify the possible dimerization suggested by the binding data, BRET² experiments were performed, by expressing constant amounts of RXFP2 Rluc with increasing amounts of RXFP2 GFP². Increasing BRET² signals were observed with increasing amounts of RXFP2 GFP² as shown in the saturation curves for the RXFP2 Rluc/RXFP2 GFP² pair, confirming that this receptor homodimerizes (Fig. 5A).

As recently discussed (41), careful controls are needed in the interpretation of BRET results. Therefore, control experiments for the specificity of the interaction were performed. This was done by cotransfecting RXFP2 Rluc with increasing amounts of NK1R GFP² and two membrane-inserted GFP²-tagged constructs (14aa GFP² and GFP² 17aa) (Fig. 5B). The curves, obtained with all three control unrelated competitors, were straight lines with no saturation level and showed a very weak signal within the GFP/Rluc ratio at which RXFP2 Rluc/RXFP2 GFP² pair reached saturation. Confocal fluorescence microscopy demonstrated proper membrane localization of the 14aa GFP² and GFP² 17aa constructs (supplemental Fig. 3, published as supplemental data on The Endocrine Society's Journals Online web site at http://endo.endojournals.org). Furthermore, when constant amounts of RXFP2 Rluc and -GFP² were cotransfected with increasing amounts of the wild-type (WT) RXFP2 without a tag (Fig. 5C), the BRET² signal decreased.

The fact that the curve for the RXFP2 Rluc/RXFP2 GFP² pair reached saturation level contrasts with that of the curve predicted if the observed BRET² resulted from random collisions promoted by a high receptor density. Indeed, a quasilinear curve would be expected if a BRET² signal was generated by high expression levels of GFP² (42) as was seen in the first control experiment, where RXFP2 was coexpressed

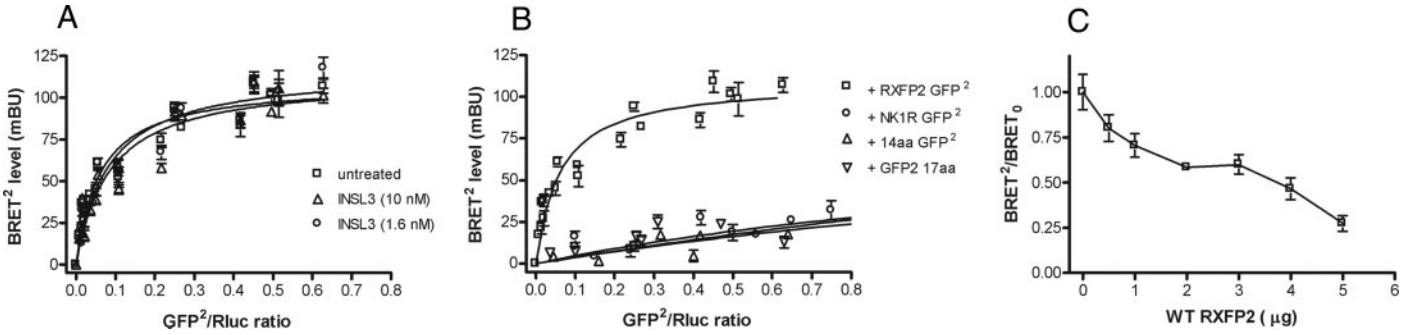

FIG. 5. BRET² results. A, Saturation curve for RXFP2. Increasing BRET² signals were observed with increasing amounts of GFP² constructs, confirming that this receptor homodimerizes. Stimulation with the agonist did not promote any consistent change in the signal. B, Control experiment for RXFP2, where the saturation curve from A (without stimulation with ligand) is compared with the curve obtained by transfecting the cells with 1 μg RXFP2 Rluc together with increasing amounts of unrelated competitors: NK1R GFP² (ranging from 0–5 μg) and two membrane-inserted GFP² constructs (14aa GFP² or GFP² 17aa ranging from 0–2 μg). The curves for the unrelated competitors are very low and show only straight lines with no saturation level. C, Another control experiment for RXFP2; 1 μg RXFP2 Rluc was coexpressed with 2 μg RXFP2 GFP² and increasing amounts of the WT RXFP2, ranging from 0–5 μg. As the amount of the WT receptor increases, the BRET² signal decreases. $BRET_0$ is the BRET² signal obtained in the absence of competitor.

together with increasing amounts of NK1R GFP² or membrane-inserted GFP²-tagged control constructs. This proves the specificity of the interaction. The second proof for the specificity is the fact that the WT RXFP2 receptor competes for the dimerization between RXFP2 Rluc and RXFP2 GFP².

Stimulation with the agonist did not promote any significant change in the BRET² signal (Fig. 5A). As a control experiment, the binding of INSL3 to both RXFP2 Rluc and RXFP2 GFP² was measured, and all constructs did bind the ligand normally (data not shown). This indicates that the receptor is present as a constitutive dimer before stimulation with the ligand as also shown previously for the β_1- and β_2-adrenergic receptors (42), for the TSH and lutropin receptors (26), and for the chemokine receptors (43). However, this is the first time that dimerization is shown for the class C of the LGR subgroup of GPCRs. One cannot exclude the possibility that agonist stimulation could promote assembly/disassembly cycles of the receptors that do not affect the steady-state fraction of receptors engaged in dimers. In contrast, transient interactions have been shown for binding of CG to the LH receptor, indicating that this receptor forms agonist-promoted dimers (40, 44).

Urizar *et al.* (26) have shown that the glycoprotein hormone receptors are able to heterodimerize, and therefore we have investigated the heterodimerization between RXFP1 and RXFP2 and showed that they do as well. The BRET² ratio for the RXFP2/RXFP1 pair was, however, slightly less than for the RXFP2 homodimerization, indicating that the homodimer is preferred (Fig. 6A), although the difference is not statistically significant. This is consistent with the result from the RXFP1/RXFP2 pair (data not shown), which showed the same BRET² ratio. Because both receptors play an important role in reproductive physiology, the heterodimerization might play a physiological role, although there is no evidence so far that they are expressed in the same cells. This will have to be investigated further.

Role of the receptor ectodomain in dimerization

Fan and Hendrickson (45) suggested that the ectodomain of the FSH receptor is responsible for dimerization of the receptor and that the 7TM domain of each receptor component would remain widely separated in the receptor dimer. This could be true for all glycoprotein hormone systems because these systems share so many common features. However, this model has been questioned (46). Moreover, Urizar *et al.* (26) showed for the TSH and the LH/CG receptors that the 7TM domain is sufficient for dimerization and that the ectodomain only stabilizes the interaction. To test whether dimerization of the RXFP2 receptor required interactions involving the ectodomain, we performed BRET² by cotransfecting HEK293 cells with a constant amount of RXFP2 Rluc with increasing amounts of a construct devoid of the N-terminal hormone-binding domain (RXFP2 TM1–7 GFP²). The expression of both the holoreceptor and the truncated form of the receptor on the cell membrane has been investigated, and both receptors are expressed in similar amounts (data not shown). A BRET² signal for the heterodimerization experiment with RXFP2 and RXFP2 TM1–7 was detected, suggesting that the 7TM domain is involved in the formation of the dimer (Fig. 6B). However, the BRET²

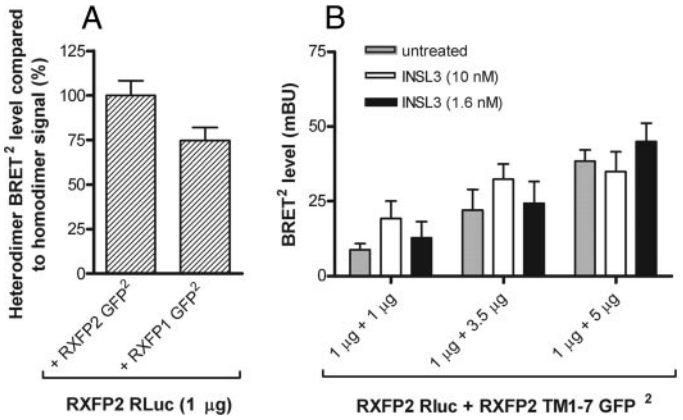

FIG. 6. Heterodimerization experiments. A, Heterodimerization between RXFP2 and RXFP1; B, heterodimerization between RXFP2 and RXFP2 TM 1–7. Cells were transfected with 1 μg RXFP2 Rluc together with either 5 μg RXFP1 GFP² (A) or increasing amounts of RXFP2 TM1–7 RXFP2 GFP² (ranging from 1–5 μg) (B).

signal was stronger for the RXFP2 holoreceptor than for the truncated form, showing that the large ectodomain seems to be involved in the stabilization of the dimer formation as well. However, the difference in the $BRET^2$ signals between the holoreceptor and the truncated form could also be due to a change in the orientation or a different distance within both $BRET^2$ pairs. The difference in the $BRET^2$ signals between the holoreceptor and the truncated form is consistent with what has been shown for the TSH receptor (26). However, the difference is more severe for the RXFP2/RXFP2 TM1–7 pair than with the TSH receptor, indicating a more substantial role of the ectodomain of the RXFP2 in the interaction. The detection of a $BRET^2$ signal is itself a confirmation that the 7TM domains must be close together (<100 Å). Liang *et al.* (47) have already shown that dimerization of rhodopsin-like GPCRs involves primarily interactions between the serpentine portions of the molecules, and this seems to be true for the LGRs as well.

We have investigated in detail for the first time the binding kinetics of a member of the LGR subclass C of the GPCRs. The results showed that binding of INSL3 to RXFP2 has many similarities but also differences in comparison with insulin binding to the insulin receptor. The temperature dependence of association and dissociation are examples of binding similarities together with the pH dependence, the occurrence of negative cooperativity, the bell-shaped dose-response curve for negative cooperativity, and the possible applicability of the cross-linking model (39). However, although the association curves for INSL3 to RXFP2 reached the same equilibrium at all temperatures, the association curves for insulin did not, due to a higher off than on rate at higher temperatures. The pH dependence was a mirror image of that seen with insulin. The difference between the dissociation with and without addition of unlabeled ligand was the opposite (supplemental data). The effect of the dose-response curve for negative cooperativity developed more slowly with INSL3 than with insulin, and the maximal effect was much lower. GPCRs were earlier believed to be monomeric, and the proposed binding model suggested that INSL3 binds to the high-affinity site in the large ectodomain of a monomer and then to the low-affinity site in the 7TM domain (12). However, the occurrence of negative cooperativity seen in our work suggested that the receptor functions as a dimer, and the bell-shaped dose-response curve for negative cooperativity suggests that the binding may happen in a *trans* rather than in a *cis* way. $BRET^2$ data validated the concept of dimerization of RXFP2 and that the 7TM domains are sufficient for dimerization. However, the ectodomains appear to be involved in dimerization as well. If the *trans*-binding model is correct, it could have interesting implications for the development of agonists and antagonists for the treatment of diseases connected to dysfunction of the relaxin signaling pathways. The relaxin and INSL3 systems have evolved only recently in evolution and may therefore not be linked to essential core functions but may rather have an add-on function. Therefore, relaxin and INSL3 might be ideal targets for novel drug development because they are expected to have few unwanted side effects (48). The elucidation of the binding mechanism is the first step in understanding the function of this hormone.

Acknowledgments

Dr. Søren Andersen from the Department of Biostatistics, Clinical and Non-Clinical, at Novo Nordisk A/S, is gratefully acknowledged for his careful statistical analysis of the data.

Received March 30, 2007. Accepted November 26, 2007.

Address all correspondence and requests for reprints to: Jane Nøhr, Ph.D, Receptor Systems Biology Laboratory, Hagedorn Research Institute, Niels Steensens Vej 6, DK-2820 Gentofte, Denmark. E-mail: jnql@novonordisk.com.

This work was supported by Australian National Health and Medical Research Council (NHMRC) Project Grants 30012 and 350245 (to J.D.W. and R.A.D.B.) and by the Slovenian Research Agency/Slovenian-Danish collaboration Grant BI-DK/06-07-007) (to M.V.).

The Receptor Systems Biology Laboratory and the Hagedorn Research Institute are independent basic research components of Novo Nordisk A/S.

Present address for T.M.E.: University of Florida College of Medicine, P.O. Box 100793, Gainesville, Florida 32601.

Disclosure Statement: The authors have nothing to disclose.

References

1. **Roche PJ, Butkus A, Wintour EM, Tregear GW** 1996 Structure and expression of Leydig insulin-like peptide mRNA in the sheep. Mol Cell Endocrinol 121: 171–177
2. **Wilkinson TN, Speed TP, Tregear GW, Bathgate RA** 2005 Evolution of the relaxin-like peptide family. BMC Evol Biol 5:14
3. **Bathgate RAD, Samuel CS, Burazin TC, Gundlach AL, Tregear GW** 2003 Relaxin: new peptides, receptors and novel actions. Trends Endocrinol Metab 14:207–213
4. **Bathgate RAD, Hsuch AJW, Sherwood OD** 2005 Physiology and molecular biology of the relaxin peptide family. In: Neill J, Wassarmann P, eds. Knobil and Neill Physiology of reproduction. Philadelphia: Elsevier; 679–768
5. **Adham IM, Burkhardt-Goettges E, Engel W** 1996 The Leydig insulin-like peptide. J Anim Breed Genet 113:229–235
6. **De Meyts P** 2004 Insulin and its receptor: structure, function and evolution. Bioessays 26:1351–1362
7. **Buellesbach EE, Yang S, Schwabe C** 1992 The receptor-binding site of human relaxin II: a dual prong-binding mechanism. J Biol Chem 267:22957–22960
8. **Buellesbach EE, Schwabe C** 1995 A novel Leydig cell cDNA-derived protein is a relaxin-like factor. J Biol Chem 270:16011–16015
9. **Buellesbach EE, Schwabe C** 1994 Functional importance of the A chain loop in relaxin and insulin. J Biol Chem 269:13124–13128
10. **Claasz AA, Bond CP, Bathgate RAD, Otvos L, Dawson NF, Summers RJ, Tregear GW, Wade JD** 2002 Relaxin-like bioactivity of ovine insulin 3 (INSL3) analogues. Eur J Biochem 269:6287–6293
11. **Rosengren KJ, Zhang S, Lin F, Daly NL, Scott DJ, Hughes RA, Bathgate RAD, Craik DJ, Wade JD** 2006 Solution structure and characterization of the LGR8 receptor binding surface of insulin-like peptide 3. J Biol Chem 281:28287–28295
12. **Halls ML, Bond CP, Sudo S, Kumagai J, Ferraro T, Layfield S, Bathgate RAD, Summers RJ** 2005 Multiple binding sites revealed by interaction of relaxin family peptides with native and chimeric relaxin family peptide receptors 1 and 2 (LGR7 and LGR8). J Pharmacol Exp Ther 313:677–687
13. **Hsu SYT, Semyonov J, Park JI, Chang CL** 2005 Evolution of the signaling system in relaxin-family peptides. Ann NY Acad Sci 1041:520–529
14. **Sudo S, Kumagai J, Nishi S, Layfield S, Ferraro T, Bathgate RA, Hsueh AJ** 2003 H3 relaxin is a specific ligand for LGR7 and activates the receptor by interacting with both the ectodomain and the exoloop 2. J Biol Chem 278: 7855–7862
15. **Halls ML, Bathgate RAD, Sudo S, Kumagai J, Bond CP, Summers RJ** 2005 Identification of binding sites with differing affinity and potency for relaxin analogues on LGR7 and LGR8 Receptors. Ann NY Acad Sci 1041:17–21
16. **De Meyts P, Roth J, Neville Jr DM, Gavin JR, Lesniak MA** 1973 Insulin interactions with its receptors, experimental evidence for negative cooperativity. Biochem Biophys Res Commun 55:154–161
17. **De Meyts P, Bianco AR, Roth J** 1976 Site site interactions among insulin receptors. Characterization of the negative cooperativity. J Biol Chem 251: 1877–1888
18. **Koshland DE Jr., Hamadani K** 2002 Proteomics and models for enzyme cooperativity. J Biol Chem 277:46841–46844
19. **Koshland Jr DE** 1996 The structural basis of negative cooperativity: receptors and enzymes. Curr Opin Struct Biol 6:757–761
20. **Limbird LE, De Meyts P, Lefkowitz RJ** 1975 β-Adrenergic receptors: evidence for negative cooperativity. Biochem Biophys Res Commun 64:1160–1168
21. **De Meyts P** 1976 Cooperative properties of hormone receptors in cell membranes. J Supramol Struct 4:241–258
22. **Powell-Jones CH, Thomas Jr CG, Nayfeh SN** 1979 Contribution of negative

cooperativity to the thyrotropin-receptor interaction in normal human thyroid: kinetic evaluation. Proc Natl Acad Sci USA 76:705–709
23. **Pollet RJ, Standaert ML, Haase BA** 1980 Hormone-receptor interactions are noncooperative: application to the β-adrenergic receptor. Proc Natl Acad Sci USA 77:4340–4344
24. **Springael JY, Urizar E, Costagliola S, Vassart G, Parmentier M** 2007 Allosteric properties of G protein-coupled receptor oligomers. Pharmacol Ther 115:410–418
25. **Angers S, Salahpour A, Joly E, Hilairet S, Chelsky D, Dennis M, Bouvier M** 2000 Detection of β2-adrenergic receptor dimerization in living cells using bioluminescence resonance energy transfer (BRET). Proc Natl Acad Sci USA 97:3684–3689
26. **Urizar E, Montanelli L, Loy T, Bonomi M, Swillens S, Gales C, Bouvier M, Smits G, Vassart G, Costagliola S** 2005 Glycoprotein hormone receptors: link between receptor homodimerization and negative cooperativity. EMBO J 24:1954–1964
27. **Bathgate RAD, Lin F, Hanson NF, Otvos L, Guidolin A, Giannakis C, Bastiras S, Layfield SL, Ferraro T, Ma S, Zhao CX, Gundlach AL, Samuel CS, Tregear GW, Wade JD** 2006 Relaxin-3: improved synthesis strategy and demonstration of its high-affinity interaction with the relaxin receptor LGR7 both in vitro and in vivo. Biochemistry 45:1043–1053
28. **Wolven A, Okamura H, Rosenblatt Y, Resh MD** 1997 Palmitoylation of p59fyn is reversible and sufficient for plasma membrane association. Mol Biol Cell 8:1159–1173
29. **Hancock JF, Cadwallader K, Paterson H, Marshall CJ** 1991 A CAAX or a CAAL motif and a second signal are sufficient for plasma membrane targeting of ras proteins. EMBO J 10:4033–4039
30. **Roth J** 1975 Methods for assessing immunologic and biologic properties of iodinated peptide hormones. Methods Enzymol 37(Pt B):223–233
31. **Buellesbach EE, Schwabe C** 1999 Specific, high affinity relaxin-like factor receptors. J Biol Chem 274:22354–22358
32. **Gavin JR, Gorden P, Roth J, Archer JA, Buell DN** 1973 Characteristics of the human lymphocyte insulin receptor. J Biol Chem 248:2202–2207
33. **Vrecl M, Drinovec L, Elling C, Heding A** 2006 Opsin oligomerization in a heterologous cell system. J Recept Signal Transduct Res 26:505–526
34. **Vrecl M, Joergensen R, Pogacnik A, Heding A** 2004 Development of a BRET2 screening assay using β-arrestin 2 mutants. J Biomol Screen 9:322–333
35. **Heding A** 2004 Use of the BRET 7TM receptor/β-arrestin assay in drug discovery and screening. Expert Rev Mol Diagn 4:403–411
36. **Vrecl M, Anderson L, Hanyaloglu A, McGregor AM, Groarke AD, Milligan G, Taylor PL, Eidne KA** 1998 Agonist-induced endocytosis and recycling of the gonadotropin-releasing hormone receptor: effect of β-arrestin on internalization kinetics. Mol Endocrinol 12:1818–1829
37. **Limbird LE, Lefkowitz RJ** 1976 Negative cooperativity among β-adrenergic receptors in frog erythrocyte membranes. J Biol Chem 251:5007–5014
38. **De Meyts P, Whittaker J** 2002 Structural biology of insulin and IGF1 receptors: implications for drug design. Nat Rev Drug Discov 1:769–783
39. **De Meyts P** 1994 The structural basis of insulin and insulin-like growth factor-I receptor binding and negative co-operativity, and its relevance to mitogenic versus metabolic signalling. Diabetologia 37:S135–S148
40. **Ji I, Lee C, Song Y, Conn PM, Ji TH** 2002 *Cis*- and *trans*-activation of hormone receptors: the LH receptor. Mol Endocrinol 16:1299–1308
41. **James JR, Oliveira MI, Carmo AM, Iaboni A, Davis SJ** 2006 A rigorous experimental framework for detecting protein oligomerization using bioluminescence resonance energy transfer. Nat Methods 3:1001–1006
42. **Mercier JF, Salahpour A, Angers S, Breit A, Bouvier M** 2002 Quantitative assessment of β1- and β2-adrenergic receptor homo- and heterodimerization by bioluminescence resonance energy transfer. J Biol Chem 277:44925–44931
43. **Springael JY, Le Minh PN, Urizar E, Costagliola S, Vassart G, Parmentier M** 2006 Allosteric modulation of binding properties between units of chemokine receptor homo- and hetero-oligomers. Mol Pharmacol 69:1652–1661
44. **Ji I, Lee C, Jeoung M, Koo Y, Sievert GA, Ji TH** 2004 *Trans*-activation of mutant follicle-stimulating hormone receptors selectively generates only one of two hormone signals. Mol Endocrinol 18:968–978
45. **Fan QR, Hendrickson WA** 2005 Structure of human follicle-stimulating hormone in complex with its receptor. Nature 433:269–277
46. **Moyle WR, Lin W, Myers RV, Cao D, Kerrigan JE, Bernard MP** 2005 Models of glycoprotein hormone receptor interaction. Endocrine 26:189–205
47. **Liang Y, Fotiadis D, Filipek S, Saperstein DA, Palczewski K, Engel A** 2003 Organization of the G protein-coupled receptors rhodopsin and opsin in native membranes. J Biol Chem 278:21655–21662
48. **Ivell R, Bathgate RA** Neohormone systems as exciting targets for drug development. Trends Endocrinol Metab 17:123

***Endocrinology* is published monthly by The Endocrine Society (http://www.endo-society.org), the foremost professional society serving the endocrine community.**